Atmos. Chem. Phys. Discuss., 10, 30893–30925, 2010
www.atmos-chem-phys-discuss.net/10/30893/2010/
doi:10.5194/acpd-10-30893-2010

Atmospheric Chemistry and Physics Discussions

Attributing and quantifying European carbon monoxide sources affecting the Eastern Mediterranean: a combined satellite, modelling, and synoptic analysis study

R. Drori[1], U. Dayan[1], D. P. Edwards[2], L. K. Emmons[2], and C. Erlick[3]

[1]Department of Geography, The Hebrew University of Jerusalem, Jerusalem, Israel
[2]National Center for Atmospheric Research, Boulder, CO, USA
[3]Fredy and Nadinne Herrmann Institute of Earth Sciences, The Hebrew University of Jerusalem, Jerusalem, Israel

Received: 29 October 2010 – Accepted: 25 November 2010 – Published: 21 December 2010

Correspondence to: R. Drori (ron.drori@mail.huji.ac.il)

Published by Copernicus Publications on behalf of the European Geosciences Union.

Abstract

European pollutants are known to affect the Eastern Mediterranean (EM). However, there has been no previous study explicitly locating the European sources, characterizing their transport pathways, and quantifying their contribution to local concentrations in the EM. In the current study, spatially tagged carbon monoxide was used as a tracer for pollutant transport from Europe to the EM over five consecutive years (2003–2007) using the global chemical transport model MOZART-4. The model results were compared against NOAA/GMD ground station data and remotely sensed data from the Terra/MOPITT satellite and found to agree well. European anthropogenic emissions were found to significantly influence EM surface concentrations, while European biomass burning (BB) emissions were found to have only a small impact on EM surface concentrations. Over the five simulated years, only two European biomass burning episodes contributed more than 10 ppb to surface CO concentrations in the EM. CO enhancement in the EM during the summer was attributed to synoptic conditions prone to favorable transport from Turkey and Eastern Europe towards the EM rather than increased emissions. We attribute the apparently misleading association between CO emitted from European BB and CO enhancements over the EM to typical summer synoptic conditions caused by the lingering of an anticyclone positioned over the Western and Central Mediterranean Basin that lead to forest fires in the area. Combined with a barometric trough over the eastern part of the Mediterranean Basin, this generates a prevailing transport of air masses from Eastern Europe to the EM shore.

1 Introduction

Numerous studies have shown that gas phase pollution and airborne particulate matter from European sources travel over the Mediterranean Sea downwind to the Eastern Mediterranean (EM) region (Luria et al., 1996; Wanger et al., 2000; Lelieveld, et al., 2002; Matvev et al., 2002; Dayan and Levy, 2005; Erel et al., 2007). Transport of

ACPD
10, 30893–30925, 2010

pollution from Europe to the EM is controlled by the wind flow resulting from a combination of synoptic systems, the one formed over Europe in tandem with those located over the EM. Evidence for contamination of lower tropospheric layers over the EM by pollution emitted from European sources during summer has been shown (Dayan and Graber, 1981; Dayan and Levy, 2005; Koch and Dayan, 1992; Dayan et al., 2002). However, locating the European sources affecting the EM, characterizing their transport pathways, and quantifying their contribution to local concentrations has not yet been accomplished. In this study, we use carbon monoxide (CO) as a tracer for European pollutants. CO has a global-average lifetime of about two months and its molecular weight is close to that of air. It is therefore widely used as a tracer to track pollution transport and to quantify the contribution of source emissions to local concentrations (Edwards et al., 2004; Pfister et al., 2004; Duncan et al., 2007). In addition to chemical oxidation in the atmosphere, CO is emitted from both anthropogenic and biomass burning (BB) sources (additional sources are vegetation and ocean). The CO seasonal cycle is mainly governed by the concentration of OH (Novelli et al., 1992) and is expected to be lowest in the late summer and highest during late winter or spring.

We aim to identify and quantify European CO sources contributing to surface concentration over the EM region, to characterize the synoptic conditions leading to significant pollutants transport from Europe to the EM, and to assess the relative importance and impacts of anthropogenic and BB sources to EM CO concentrations. In order to gain better insight into the mechanisms leading to European CO transport to the EM and to quantify the different source contributions, we make use of numerical simulations, in situ and remote sensing observations, and synoptic analyses. The chemical transport model MOZART-4 is used to locate and quantify the contribution of European sources to local concentrations over the EM. The model results are compared to measurements from a ground monitoring station and retrievals from the MOPITT satellite instrument. A synoptic classification scheme is used to characterize significant pollution events and to identify transport circulation patterns from Europe to the EM.

ACPD
10, 30893–30925, 2010

The paper is organized as follows: in Sect. 2 we introduce the MOZART-4 model, the emissions inventory used and a brief description of the concept of tagged runs. In Sect. 3, after a description of Measurements of Pollution in the Troposphere (MOPITT) and NOAA Earth System Research Laboratory Global Monitoring Division flask measurements (ESRL/GMD), the model results are evaluated with MOPITT and GMD ground station data. In Sect. 4, the model results are used to locate the European sources affecting the EM, and the contribution of each source to local concentrations is discussed. In Sect. 5, we characterize the synoptic configuration leading to significant transport episodes. In Sect. 6, we discuss the relative importance of anthropogenic and BB sources, and finally we present the main conclusions in Sect. 7.

2 Model description

2.1 MOZART-4

The Model for Ozone and Related chemical Tracers, version 4 (MOZART-4) is a global chemical transport model of the troposphere (Emmons et al., 2010). For this study, the tracer version of MOZART-4 is used, where only CO is simulated. CO sources include direct emissions and secondary production from the oxidation of hydrocarbons, while CO sinks include reaction with OH and dry deposition. Monthly averages of OH and CO chemical production fields (from CH_4 and other hydrocarbon oxidation) are taken from a previous simulation with full chemistry. The dry deposition scheme from Sanderson et al. (2003) is included in MOZART-4. The model is driven by meteorological inputs from the National Centers for Environmental Prediction/National Center for Atmospheric Research NCEP/NCAR Reanalysis with time steps of 6 h (Kalnay et al., 1996). A horizontal resolution of 2.8° in latitude by 2.8° in longitude is used with 28 sigma levels extending from the surface up to a pressure level of about 2 hPa. The model is run in time steps of 20 min. The simulated mixing ratios of CO and each tag are averaged over 24 h.

ACPD
10, 30893–30925, 2010

2.2 CO emissions

Anthropogenic pollutants are emitted principally from fixed sources, such as urban or industrial areas, or from specific known locations, such as roads. Although there is evidence that European anthropogenic emissions may be decreasing (Meszaros et al., 2005), we assumed a constant annual anthropogenic surface emission flux of CO, using the values for the year 2005 as obtained from the Precursors of Ozone and their Effects in the Troposphere (POET) inventory (Granier et al., 2005).

BB emissions, on the other hand, exhibit large spatial and temporal variability (Edwards et al., 2004) and are characterized by large uncertainties in timing, location, and magnitude (Bian et al., 2007). Furthermore, synoptic scale transport is very sensitive to the timing and location of emissions (Ranmar et al., 2002; Dayan and Levy, 2002, 2005; Dayan and Lamb, 2007). Chen et al. (2009) applied three BB inventories with different temporal resolutions: monthly from Global Fire Emissions Database version 2 (GFEDv2), 8-day (GFEDv2 resampled with MODIS 8-day fire counts), and daily (GFED 8-daily resampled using the GOES ABBA diurnal cycle). They compared the model results with satellite, aircraft, and ground based measurements and concluded that, "switching from monthly to 8-day time intervals for emissions has the largest effect on CO and aerosol distributions, and shows better agreement with measured day-to-day variability". In the absence of a daily inventory, we used the 8-day fire emissions from the Global Fire Emissions Database version 2 (van der Werf et al., 2006). This inventory was resampled from the monthly GFED 2 inventory to an 8-day time step using Moderate Resolution Imaging Spectroradiometer (MODIS) fire hot spots (Giglio et al., 2003).

2.3 The concept of tagged runs

CO has a principal chemical sink, the OH radical, and therefore can be simulated linearly. CO sources can be tagged according to their type (e.g., anthropogenic or BB), location (e.g., East or West Europe), and timing (e.g., month of the emissions). Each

ACPD
10, 30893–30925, 2010

of these tagged CO sources is treated as a separate "species" and can be used as a tracer to identify transport pathways and to evaluate the contribution of each source to local CO total concentration. Here we spatially tag the European CO sources and separate them into two types, BB and anthropogenic sources. For each source type, six areas ("tags") are defined, making a total of 12 tags for the whole continent. The six regions that were tagged for each source type are shown in Fig. 1: South Western Europe (tag 1), Balkans (tag 2), Turkey and Eastern Europe (tag 3), North Western Europe (tag 4), North Eastern Europe (tag 5), and Eastern Mediterranean (tag 6). The tags were defined according to known transport pathways (Erel et al., 2007; Dayan and Levy, 2005) and emission spatial distributions according to the POET and GFED inventories.

3 Model results and evaluation

3.1 Model results

The time series of CO surface concentration for a MOZART grid cell centered over 32.85° N and 33.75° E between 2003 and 2007 is shown in Fig. 2. The seasonal cycle can be seen, with high CO concentration during winter months, reaching a maximum in spring, and decreasing sharply around May. The CO concentration for the mid-summer months (i.e., July and August) is higher than in the early summer (i.e., May–June). Another decrease in concentration can be seen in September and October followed by a sharp increase during November and December. A similar pattern is exhibited by the five year averaged CO (Fig. 3). CO variability during autumn, winter, and spring is much higher than in the summer, reflecting the synoptic variability during these months compared with the stable atmospheric conditions characterizing the summer. CO originating from chemical production rather than direct emissions tends to have a small interannual variability (simulation not shown here), with peaks ranging between 50 and

ACPD
10, 30893–30925, 2010

70 ppb. These values can contribute more than 50% to local surface concentrations of CO during the summer.

3.2 Comparison of the model to MOPITT observations

Measurements Of Pollution In The Troposphere (MOPITT), onboard the Terra satellite, is an eight-channel gas correlation radiometer with pixel resolution of about 22 km by 22 km at nadir and a swath width of about 640 km. Global coverage is achieved in about three days under clear sky conditions. Version 4 MOPITT level 2 CO retrievals are used in this study (Deeter et al., 2010). The MOPITT retrievals include the CO mixing ratio for ten atmospheric levels from the surface to 100 hPa with 100-hPa grid spacing and the total column amount of CO in the atmosphere. MOPITT retrievals are based on the Maximum a Posteriori (MAP) technique incorporating a priori information about the CO profile and its covariance (Deeter et al., 2003). Each of the retrievals is associated with an "averaging kernel" matrix which indicates the sensitivity of MOPITT measurements to the true CO profile. In addition, the "Degrees of Freedom for Signal" (DFS), which is the trace of the averaging kernel matrix, is given. The DFS describes the number of pieces of independent information contained in the retrieved profile. A low DFS value indicates that the retrieval is mainly based on a priori data and not on measurement. The range of DFS values associated with MOPITT thermal infrared retrievals span between 0 and 2 (Deeter et al., 2004). DFS values over the EM are relatively high and span between 1 and 2. MOPITT measurements rely on thermal contrast between the surface and atmosphere and therefore are mainly sensitive to the free troposphere with only limited surface sensitivity (Edwards et al., 2004).

To properly compare MOZART with MOPITT products, the averaging kernel and a priori profile associated with each of the MOPITT retrievals must be applied to the model profiles (Emmons et al., 2009a).

ACPD
10, 30893–30925, 2010

MOPITT data used in this study were filtered using the following criteria:

1. For a better surface sensitivity, only daytime retrievals were used since larger thermal contrast is expected during the day, and weighting functions generally peak lower in the atmosphere in the daytime.

2. In order to avoid comparison of sparse MOPITT measurements (22-km horizontal resolution) and the coarse grid of the MOZART model (2.8°), only passes that fill more than half the area of a MOZART grid cell are considered.

A comparison of MOZART to MOPITT CO retrievals is shown in Fig. 4. Overall there is good agreement, and the model successfully reproduces the daily CO variations ($0.729 < R < 0.89$; $5 < \text{Bias} < 11$ ppb).

3.3 Evaluation of the model with GMD ground station data

Unfortunately, only one background monitoring ground station located in the southern EM is available over the whole EM region. The CO in situ observations are extracted from the Israeli NOAA Global Monitoring Division (GMD) site at Sde-Boker (31.13° N, 34.88° E, 400 m a.s.l.) operated by the Weizmann Institute of Science. CO surface concentration is measured on a weekly basis at Sde-Boker as part of the NOAA/GMD flask sampling program (Novelli et al., 1992, 1998, 2010).

A comparison of MOZART simulated CO concentrations (960 hPa at Sde-Boker) to the GMD station data from Sde-Boker (southern MOZART grid cell) is shown in Fig. 5. The model generally reproduces both the magnitude and variability of CO concentrations well, with an overall correlation ranging from 0.53 to 0.71 and an overall bias ranging from 0 to 14 ppb. The lower end of the correlation values and the higher end of the bias values come from the spring months (March–May) of 2003. A possible explanation for the discrepancy between the model and measurements in the spring of 2003 is the presence of widespread European forest fires that existed during that season; since fire-induced plume rise is not included in the simulations. The correlation for the

ACPD
10, 30893–30925, 2010

years 2004–2007 alone is relatively high, ranging from 0.61 to 0.71 and the bias for 2004–2007 is minimal, ranging from 0 to 2.6 ppb.

3.4 Comparison of MOPITT retrievals with GMD ground station data

This study is focused on the contribution of European CO sources to local surface concentrations and therefore it would be beneficial to evaluate MOPITT low level retrievals with ground station measurements.

MOPITT version 4 data is less sensitive to surface concentrations and therefore generally cannot be compared directly to ground station measurements in a quantitative manner (Deeter et al., 2010). However, at an arid location (such as Sde-Boker, located in the Negev Desert), where there is high thermal contrast near surface during the day, the MOPITT weighting functions have lower peaks, allowing better sensitivity near surface. (Note however, that this does not mean that the MOPITT retrieval represents the surface concentration but rather an average value from surface to the mid-free troposphere). Due to the coarse temporal resolution of both MOPITT and the GMD station, only monthly means are compared here. A comparison between MOPITT monthly mean CO at 900 hPa and GMD monthly mean CO measurements is shown in Fig. 6. The MOPITT and GMD data are well correlated, with a correlation varying from 0.66 to 0.82. This is a qualitative comparison and therefore the bias is not given.

4 European CO sources affecting the EM region

The contribution of European emissions to local CO surface concentrations is comparable to that from local (tag 6) emissions (Fig. 7). European sources can contribute up to 90 ppb. High contributions are seen mainly during the winter months, peaking in March. The seasonal cycle of the European contribution is very similar to the seasonal cycle of total CO, with a high concentration in winter, spring, and autumn and a lower concentration in summer.

ACPD
10, 30893–30925, 2010

The average contribution of each anthropogenic tag to the local surface concentration is shown in Fig. 8. Anthropogenic European emissions significantly affect the Eastern Mediterranean. All anthropogenic tags, except south western Europe (tag 1), contribute year-round. The highest contribution is from Turkey and Eastern Europe (tag 3). Central Europe (tag 2) and Northern Europe and Western Europe (tags 4 and 5) are found to contribute mainly during the winter and spring. While the average tag contribution ranges between 5 and 15 ppb, extreme episodes of more than 40 ppb were simulated (not shown here). Local and European emission contributions to local CO concentrations are generally negatively correlated, meaning that either local or European sources are dominant (Fig. 7), except in the summer, when both local and European sources are simultaneously affect the local CO concentration. A possible explanation for the positive correlation in the summer is the short range of air mass transport during summer caused by the dominant synoptic system for this season, i.e., the Persian trough in its weak mode recirculating local and European emissions (discussed further in Sect. 5). European CO variability during winter is much higher than in the summer due to the stable nature of the EM summer. The European contribution is usually lower than the local contribution during autumn and higher than the local contribution during winter, mainly due to the difference in wind flow (mainly northerly, preventing transport, during the autumn versus mainly westerly during winter).

5 Synoptic conditions leading to significant pollution transport from Europe to the EM

Several studies have presented strong evidence for contamination of lower tropospheric layers over the EM by pollution emitted from European sources during the summer (Dayan and Graber, 1981; Dayan and Levy, 2005; Koch and Dayan, 1992; Dayan et al., 2002). The synoptic condition prevailing during the summer (mid-May to mid-September) over the EM is characterized by the predominance of a thermal low-pressure trough extending from the southwest Asian Monsoon, known as the "Persian

ACPD
10, 30893–30925, 2010

Trough" (PT). This trough is confined to shallow atmospheric layers (up to about 1000 m a.s.l.) and advects cool and moist air on shore leading to a persistent elevated marine inversion. The PT is capped by much warmer and subsiding dry air of a subtropical high-pressure system centered over North Africa and the EM. In the deep PT mode, a steep pressure gradient is built, stronger westerly winds and cooler temperatures prevail over the EM, and higher concentrations of trace gases from European origin are observed in the EM atmosphere (Erel et al., 2007).

Here we will examine the synoptic conditions for episodes in which a European tag contribution of 20 ppb is exceeded (a threshold equivalent to about 10% of the highest local CO surface concentration) and consequently has contributed significantly to an elevated CO concentration over the EM.

Attributing CO pathways to synoptic circulation patterns must be done carefully for the following reasons:

1. Synoptic systems over the EM tend to have a relatively small spatial extent and often develop in conjunction with different synoptic systems over Europe; EM synoptic systems alone cannot explain the variation in European source contributions.

2. CO has a long residence time relative to the synoptic time scale. CO emitted from Europe can be recirculated for several weeks over the EM and therefore cannot always be attributed to a single synoptic system or source.

To overcome these challenges, we have used a classification scheme that combines the widely used synoptic classification of Alpert et al. (2004) for representing local conditions with back trajectory analysis for upwind European meteorological conditions.

We performed classification for each day using the NCEP/NCAR Sea Level Pressure SLP field at 12:00 UTC and the synoptic categories adopted from Alpert et al. (2004), as listed in Table 1. Five-day back-trajectories were calculated for each day for 2003 using the HYSPLIT model (Draxler et al., 2003). The trajectories were classified into 10 clusters using HYSPLIT standard clustering analysis (Fig. 9). HYSPLIT cluster analysis is a hierarchal clustering algorithm seeking to minimize the Euclidean distance

ACPD
10, 30893–30925, 2010

between all trajectories in the same cluster. For each day, the corresponding cluster was associated with a synoptic classification. The frequency (in days) for each possible combination of synoptic system and back-trajectory cluster for 2003 is shown in Fig. 10.

To elucidate the advantage of this methodology over traditional synoptic system classifications, the most frequent synoptic system over the EM, namely the weak Persian trough (WPT), was further analyzed. The WPT system is very common during summer over the EM, causing local north-west winds. During the summer of 2003, more than 80 days were classified as WPT. From Fig. 10, the WPT is associated with almost all trajectory clusters. The three main back-trajectories cluster associated with WPT are cluster 7 (Balkans, tag 3, 43 cases), cluster 6 (Western Europe, tag 4, 7 cases) and cluster 5 (Eastern Europe, tag 3, 14 cases). SLP composites of each WPT sub-class along with the corresponding mean back-trajectory cluster are shown in Fig. 11, illustrating the difference between these subtypes. The difference in pathways is attributed to differences in the horizontal pressure gradient over the EM's synoptic system and differences in the location and strength of the anticyclone over Europe.

Results from the combination of synoptic system with back-trajectory cluster for 2003 (Fig. 10) indicates that emissions from Central Europe (tag 2) mainly contribute during the winter months, with some contribution during the summer and autumn. The high European contribution for this region (2) is associated with trajectory clusters 6 and with cyclone activity over the EM or a high barometric pressure system to the north. Eastern Europe contributes all year round, except during late spring and autumn. The main trajectories during May and October are of relatively short range (trajectories 1, 7 and 8) and are mainly associated with a high over the EM region. Northwest Europe (tag 4) contributes mainly during the winter and autumn under similar conditions as described for tag 2. Northeast Europe (tag 5) contributes mainly during the winter and has a strong association with a high pressure from the north (the Siberian high). No distinct trajectory is associated with this source (5, 7, 8, 9, and 10).

ACPD
10, 30893–30925, 2010

6 The relative importance of European anthropogenic and BB sources to EM near surface concentrations

The flux of European BB carbon monoxide emissions from some areas of Europe is comparable to the flux of anthropogenic CO emissions and may even exceed the latter during extreme BB episodes (GFED2 and POET inventories; Fig. 12). Furthermore, there is some correlation between European BB emissions and EM CO concentrations (Fig. 13). However, the European BB contribution to local surface CO concentrations in the EM is actually small. Over the five years simulated, only two cases of significant contribution were detected. The first case is at the end of April 2006, when widespread agriculture fires occurred over Northern Russia (tag 5). The second case is at the end of August 2007, when huge fires occurred over Greece (tag 2). While local CO enhancement is correlated with the respective BB episodes over Europe, model results indicate that anthropogenic emission from tag 3 is the cause for these elevated values.

A possible explanation for the minor contribution of European BB to local surface CO concentrations in the EM is the change in synoptic conditions over the Mediterranean basin during summer, when most of the biomass burning occurs. The typical synoptic condition during summer over the EM is a weak or moderate Persian trough. Under these synoptic systems, air masses travel to the EM coast from the Mediterranean basin or Turkey (tag 3) with northwesterly winds (trajectories 5 and 7). At the same time, a clock-wise flow around an anticyclone located over central Mediterranean transports European pollutants southwesterly. An NCEP/NCAR SLP composite of all days that have been identified as WPT with trajectory 7 is shown in Fig. 14. Average fire radiative power (a measure of the rate of radiant heat output from a fire and a proxy for BB emissions) derived from the MODIS active fire product (Giglio et al., 2003) was calculated for these days and is presented as colored rectangles. From Fig. 14, we can see why BB sources do not contribute to the EM region. Two high pressure systems coexist with the WPT: one, over western and central Europe, the second, over Russia leading to favorable meteorological conditions for widespread forest fires. This

ACPD
10, 30893–30925, 2010

synoptic configuration leads to a short back-trajectory from Turkey towards the EM advecting anthropogenic pollution (tag 3) but blocking BB emissions.

7 Summary and conclusions

The chemical transport model MOZART-4 was used to locate and quantify the impact of European CO emissions on CO surface concentrations in the Eastern Mediterranean. Model results were compared against MOPITT retrievals and ground monitoring station data and found to agree well. Selected transport events were analyzed and explained while using a methodology merging back trajectories and synoptic classification.

Our main conclusions are:

1. Anthropogenic European CO emissions contribute up to 90 ppb or about 50% of the surface CO concentration in the EM and are comparable to the contribution of local CO emissions.

2. The anthropogenic CO sources with the highest contribution to EM CO concentrations are from Turkey and Eastern Europe. Emissions from Eastern Europe contribute throughout the year to EM CO concentrations with the exception of late spring and autumn. Emissions from Central Europe mainly contribute during the winter months with a lesser contribution during summer and autumn.

3. CO measurements, both in situ and remotely sensed, as well as modeled CO; indicate an enhancement of CO concentrations in the EM during summer, as opposed to the expected minima during summer. This enhancement is attributed to typical summer synoptic conditions rather than emission enhancement (such as European BB).

4. European BB contribution to EM surface concentration is minimal. Typical synoptic summer conditions lead to north westerly winds over the EM, advecting CO

ACPD
10, 30893–30925, 2010

from Turkey (tag 3). At the same time, a clock-wise flow around an anticyclone located over Western and Central Europe transports European BB south westerly.

This paper represents the first attempt to quantify the contribution of various European CO sources to EM surface concentration and to characterize transport patterns using a new synoptic classification scheme. The combination of model simulation, in situ and remotely sensed data and synoptic analysis enable us to analyze European source contributions and characterize flow patterns on a daily basis and to assess the importance of each source on a relatively small spatial scale. This methodology could also be adopted for other areas and for other pollutants. Limitations of the current work, and areas that will be explored in the future, include a more comprehensive synoptic analysis covering more than one year and an improved modeling of pyroconvection and BB plume transport.

Acknowledgements. We acknowledge the work of the NOAA GMD group and Weizmann Institute of Science in making in situ measurements. The authors gratefully acknowledge the NOAA Air Resources Laboratory (ARL) for the provision of the HYSPLIT transport and dispersion model. The HUJI work was partially supported by the Ring Foundation. The National Center for Atmospheric Research is sponsored by the National Science Foundation.

References

Alpert, P. and Ziv, B.: The Sharav cyclone – Observations and some theoretical considerations, J. Geophys. Res., 94, 18495–18514, 1989.

Alpert, P., Osetinsky, I., Ziv, B., and Shafir, H.: Semi-objective classification for daily synoptic systems: Application to the eastern mediterranean climate change, Int. J. Climatol., 24, 1001–1011, doi:10.1002/joc.1036, 2004.

Bian, H., Chin, M., Kawa, S. R., Duncan, B., Arellano, A. and Kasibhatla, P.: Sensitivity of global CO simulations to uncertainties in biomass burning sources, J. Geophys. Res., 112, D23308, doi:10.1029/2006JD008376, 2007.

ACPD
10, 30893–30925, 2010

Chen, Y., Li, Q., Randerson, J. T., Lyons, E. A., Kahn, R. A., Nelson, D. L., and Diner, D. J.: The sensitivity of CO and aerosol transport to the temporal and vertical distribution of North American boreal fire emissions, Atmos. Chem. Phys., 9, 6559–6580, doi:10.5194/acp-9-6559-2009, 2009.

Dayan, U. and Graber, M.: Analysis of Synoptic Conditions in the Eastern Mediterranean that Led to Elevated Air Pollution Concentrations in Israel. Proceedings of the International 12th Scientific Conference of the Israel Ecological Society, The Hebrew University of Jerusalem, Israel, 12–13 May 1981, 383–397, 1981.

Dayan, U. and Lamb, D.: Influences of atmospheric circulation on the variability of wet sulfate deposition, Int. J. Climatol., 28, 1315–1324, doi:10.1002/joc.1648, 2008.

Dayan, U. and Levy, I.: Relationship between synoptic-scale atmospheric circulation and ozone concentrations over Israel, J. Geophys. Res., 107(D24), 4813, doi:2002JD002147, 2002.

Dayan, U. and Levy, I.: The influence of seasonal meteorological conditions and atmospheric circulation types on PM_{10} and visibility in Tel-Aviv, Israel, J. Appl. Meteorol., 44, 606–619, 2005.

Deeter, M. N., Emmons, L. K., Francis, G. L., Edwards, D. P., Gille, J. C., Warner, J. X., Khattatov, B., Ziskin, D., Lamarque, J. F., Ho, S. P., Yudin, V., Attie, J. L., Packman, D., Chen, J., Mao, D., and Drummond, J. R.: Operational carbon monoxide retrieval algorithm and selected results for the MOPITT instrument, J. Geophys. Res.-Atmos., 108, 4399–4409, doi:10.1029/2002jd003186, 2003.

Deeter, M. N., Emmons, L. K., Edwards, D. P., Gille, J. C., and Drummond, J. R.: Vertical resolution and information content of CO profiles retrieved by MOPITT, Geophys. Res. Lett., 31, 15112–15115, doi:10.1029/2004gl020235, 2004.

Deeter, M. N., Edwards, D. P., Gille, J. C., Emmons, L. K., Francis, G., Ho, S.-P., Mao, D., Masters, D., Worden, H., Drummond, J. R., and Novelli, P. C.: The MOPITT Version 4 CO product: algorithm enhancements, validation, and long-term stability, J. Geophys. Res., 7306–7318, doi:10.1029/2009JD013005, 2010.

Draxler, R. R. and Rolph, G. D.: HYSPLIT (HYbrid Single-Particle Lagrangian Integrated Trajectory) model access via NOAA ARL READY website: http://ready.arl.noaa.gov/HYSPLIT.php, last access: December 2010, NOAA Air Resources Laboratory, Silver Spring, MD, 2003.

ACPD
10, 30893–30925, 2010

European carbon monoxide sources affecting the Eastern Mediterranean

R. Drori et al.

Edwards, D. P., Emmons, L. K., Hauglustaine, D. A., Chu, D. A., Gille, J. C., Kaufman, Y. J., Petron, G., Yurganov, L. N., Giglio, L., Deeter, M. N., Yudin, V., Ziskin, D. C., Warner, J., Lamarque, J. F., Francis, G. L., Ho, S. P., Mao, D., Chen, J., Grechko, E. I., and Drummond, J. R.: Observations of carbon monoxide and aerosols from the terra satellite: Northern Hemisphere variability, J. Geophys. Res.-Atmos., 109, 24202–24218, 2004.

Emmons, L. K., Edwards, D. P., Deeter, M. N., Gille, J. C., Campos, T., Nédélec, P., Novelli, P., and Sachse, G.: Measurements of Pollution In The Troposphere (MOPITT) validation through 2006, Atmos. Chem. Phys., 9, 1795–1803, doi:10.5194/acp-9-1795-2009, 2009.

Emmons, L. K., Walters, S., Hess, P. G., Lamarque, J.-F., Pfister, G. G., Fillmore, D., Granier, C., Guenther, A., Kinnison, D., Laepple, T., Orlando, J., Tie, X., Tyndall, G., Wiedinmyer, C., Baughcum, S. L., and Kloster, S.: Description and evaluation of the Model for Ozone and Related chemical Tracers, version 4 (MOZART-4), Geosci. Model Dev., 3, 43–67, doi:10.5194/gmd-3-43-2010, 2010.

Erel, Y., Kalderon-Asael, B., Dayan, U., and Sandler, A.: European atmospheric pollution imported by cooler air masses to the eastern mediterranean during the summer, Environ. Sci. Technol., 41, 5198–5203, doi:10.1021/es062247n, 2007.

Giglio, L., Descloitres, J., Justice, C. O., and Kaufman, Y.: An enhanced contextual fire detection algorithm for MODIS, Remote Sens. Environ., 87, 273–282, 2003.

Granier, C., Lamarque, J. F., Mieville, A., Muller, J. F., Olivier, J., Orlando, J., Peters, J., Petron, G., Tyndall, G., and Wallens, S.: POET, a database of surface emissions of ozone precursors, available on internet at http://www.aero.jussieu.fr/projet/ACCENT/POET.php, last access: December 2010, 2005.

Kalnay, E., Kanamitsu, M., Kistler, R., Collins, W., Deaven, D., Gandin, L., Iredell, M., Saha, S., White, G., Woollen, J., Zhu, Y., Chelliah, M., Ebisuzaki, W., Higgins, W., Janowiak, J., Mo, K. C., Ropelewski, C., Wang, J., Leetmaa, A., Reynolds, R., Jenne, R., and Joseph, D.: The ncep/ncar 40-year reanalysis project, B. Am. Meteorol. Soc., 77, 437–471, 1996.

Lelieveld, J., Berresheim, H., Borrmann, S., Crutzen, P. J., Dentener, F. J., Fischer, H., Feichter, J., Flatau, P. J., Heland, J., Holzinger, R., Korrmann, R., Lawrence, M. G., Levin, Z., Markowicz, K. M., Mihalopoulos, N., Minikin, A., Ramanathan, V., de Reus, M., Roelofs, G. J., Scheeren, H. A., Sciare, J., Schlager, H., Schultz, M., Siegmund, P., Steil, B., Stephanou, E. G., Stier, P., Traub, M., Warneke, C., Williams, J., and Ziereis, H.: Global air pollution crossroads over the mediterranean, Science, 298, 794–799, 2002.

Luria, M., Peleg, M., Sharf, G., TovAlper, D. S., Spitz, N., BenAmi, Y., Gawii, Z., Lifschitz, B., Yitzchaki, A., and Seter, I.: Atmospheric sulfur over the east mediterranean region, J. Geophys. Res.-Atmos., 101, 25917–25930, 1996.

Meszaros, T., Haszpra, L., and Gelencser, A.: Tracking changes in carbon monoxide budget over Europe between 1995 and 2000, Atmos. Environ., 39, 7297–7306, 2005.

Novelli, P. C. and Masarie, K. A.: Atmospheric Carbon Monoxide Dry Air Mole Fractions from the NOAA ESRL Carbon Cycle Cooperative Global Air Sampling Network, 1988–2009, Version: 2010-07-14, 2010. Path: ftp://ftp.cmdl.noaa.gov/ccg/co/flask/event/, last access: 1 May, 2010.

Novelli, P. C., Steele, L. P., and Tans, P. P.: Mixing ratios of carbon-monoxide in the troposphere, J. Geophys. Res.-Atmos., 97(D18), 20731–20750, 1992.

Park, M., Randel, W. J., Emmons, L. K., and Livesey, N. J.: Transport pathways of carbon monoxide in the Asian summer monsoon diagnosed from Model of Ozone and Related Tracers (MOZART), J. Geophys. Res., 114, D08303, doi:10.1029/2008JD010621, 2009.

Pfister, G., Petron, G., Emmons, L. K., Gille, J. C., Edwards, D. P., Lamarque, J. F., Attie, J. L., Granier, C., and Novelli, P. C.: Evaluation of CO Simulations and the Analysis of the CO Budget for Europe, J. Geophys. Res., 109, D19304, doi:10.1029/2004JD004691, 2004.

Ranmar, D. O., Matveev, V., Dayan, U., Peleg, M., Kaplan, J., Gertler, A. W., Luria, M., Kallos, G., Katsafados, P., and Mahrer, Y.: Impact of coastal transportation emissions on inland air pollution over Israel: utilizing numerical simulations, airborne measurements, and synoptic analyses, J. Geophys. Res.-Atmos., 107, 4331–4343, doi:10.1029/2001jd000808, 2002.

Sanderson, M., Collins, W., Derwent, R., and Johnson, C.: Simulation of global hydrogen levels using a lagrangian three dimensional model, J. Atmos. Chem., 46, 15–28, 2003.

van der Werf, G. R., Randerson, J. T., Giglio, L., Collatz, G. J., Kasibhatla, P. S., and Arellano Jr., A. F.: Interannual variability in global biomass burning emissions from 1997 to 2004, Atmos. Chem. Phys., 6, 3423–3441, doi:10.5194/acp-6-3423-2006, 2006.

Wanger, A., Peleg, M., Sharf, G., Mahrer, Y., Dayan, U., Kallos, U. G., Kotroni, V., Lagouvardos, K., Varinou, M., Papadopoulos, A., and Luria, M.: Some observational and modeling evidence of long range transport of air pollutants from Europe towards the Israeli coast, J. Geophys. Res., 105(D6), 7177–7186, 2000.

ACPD
10, 30893–30925, 2010

European carbon monoxide sources affecting the Eastern Mediterranean

R. Drori et al.

Table 1. Synoptic classes.

System number	System Name
0	undefined
1	Red Sea trough with eastern axis
2	Red Sea trough with western axis
3	Red Sea trough with central axis
4	weak Persian trough
5	moderate Persian trough
6	deep Persian trough
7	high to the east
8	high to the west
9	high to the north
10	high over Israel
11	deep low to the east
12	deep Cyprus low to the south
13	shallow Cyprus low to the south
14	deep Cyprus low to the north
15	shallow Cyprus low to the north
16	cold low to the west
17	shallow low to the east
18	sharav[a] low to the west
19	sharav[a] low over Israel
20	Cole[b]
21	shallow Syrian low with high to the north

[a] Sharav cyclones, also called Saharan Depression or Kamsin Depression are the result of large-scale weak baroclinicity, enhanced by vigorous boundary-layer baroclinicity between the North African coast and the Mediterranean (Alpert and Ziv, 1989).

[b] Cole, also called saddle in a barometric map is the point where atmospheric pressure increases from both sides along one direction and decreases on both other two sides in the perpendicular direction. Like a mountain pass in a topographic map.

ACPD
10, 30893–30925, 2010

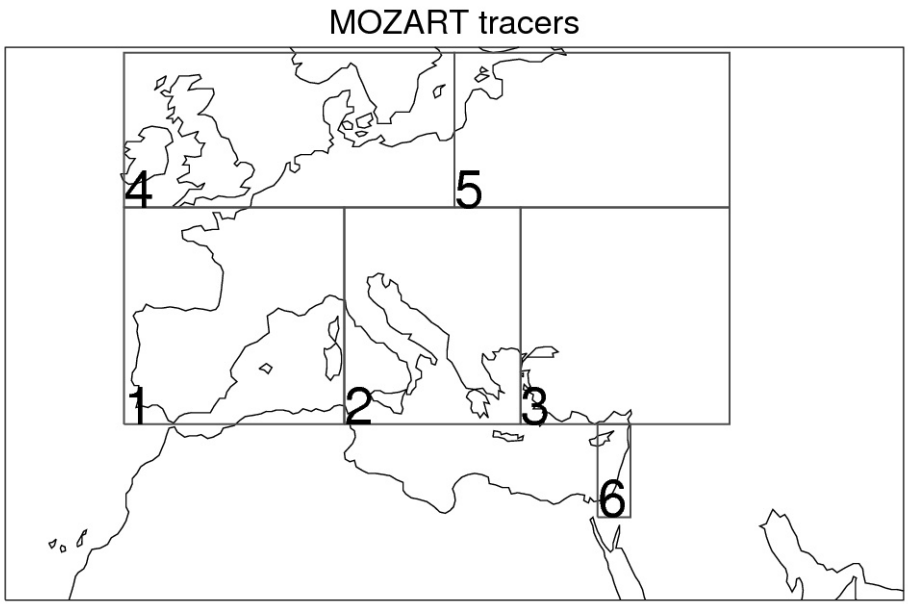

Fig. 1. Spatially tagged CO regions (both anthropogenic and BB) that were used for tracing transport in MOZART. The partitioning is based on previously known transport patterns and the emission inventory.

ACPD
10, 30893–30925, 2010

European carbon monoxide sources affecting the Eastern Mediterranean

R. Drori et al.

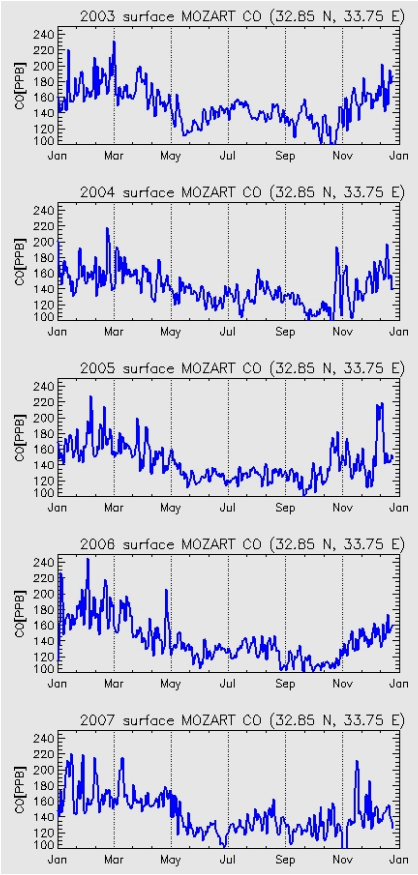

Fig. 2. MOZART-4 CO surface concentration (ppb) for the study period (2003–2007). The seasonal cycle, high CO from autumn to spring and low CO during summer, is clearly seen. CO variability from autumn to spring is much higher than during summer, reflecting the synoptic system variability during these months as opposed to the stable summer conditions.

ACPD
10, 30893–30925, 2010

European carbon monoxide sources affecting the Eastern Mediterranean

R. Drori et al.

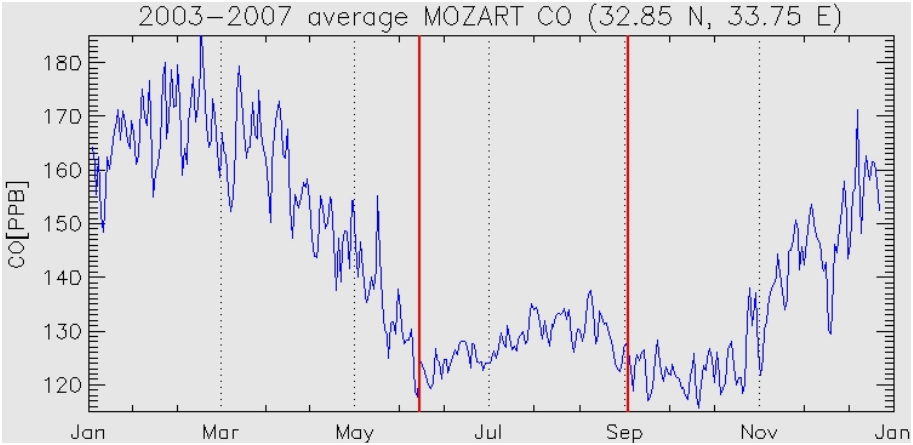

Fig. 3. Average CO surface concentrations (ppb) during the study period (2003–2007). A deviation from the expected seasonal cycle during summer can be seen (the period indicated between the red lines).

ACPD
10, 30893–30925, 2010

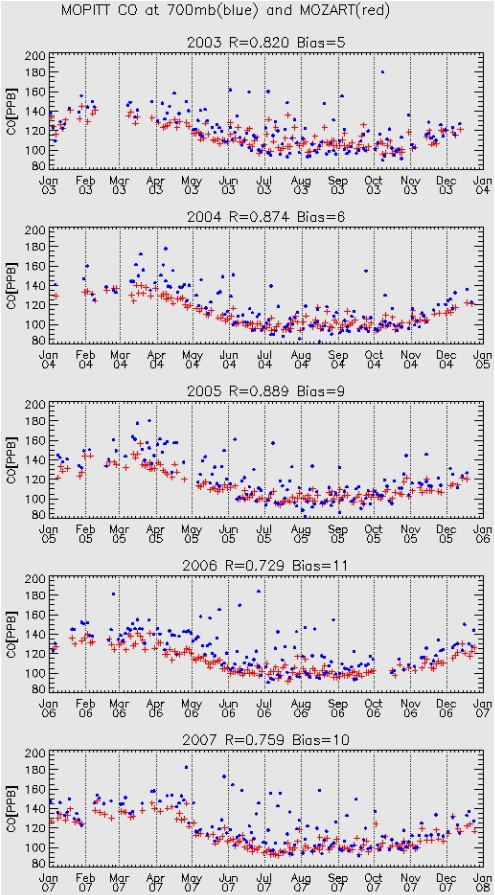

Fig. 4. Comparison of MOPITT V4 (blue dots) with MOZART (red pluses) at 700 mb, for the study period (2003–2007). The MOZART-4 results have been transformed with the MOPITT averaging kernels and a priori data.

ACPD
10, 30893–30925, 2010

European carbon monoxide sources affecting the Eastern Mediterranean

R. Drori et al.

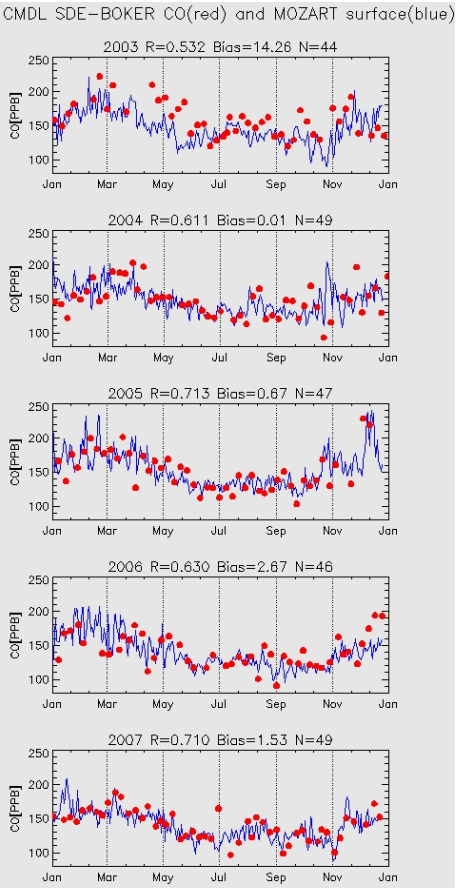

Fig. 5. Comparison of MOZART CO mixing ratio (at 960 hPa) with GMD flask measurements at Sde-Boker (31.13° N, 34.88° E, 400 m a.s.l.) for the study period (2003–2007).

ACPD
10, 30893–30925, 2010

European carbon monoxide sources affecting the Eastern Mediterranean

R. Drori et al.

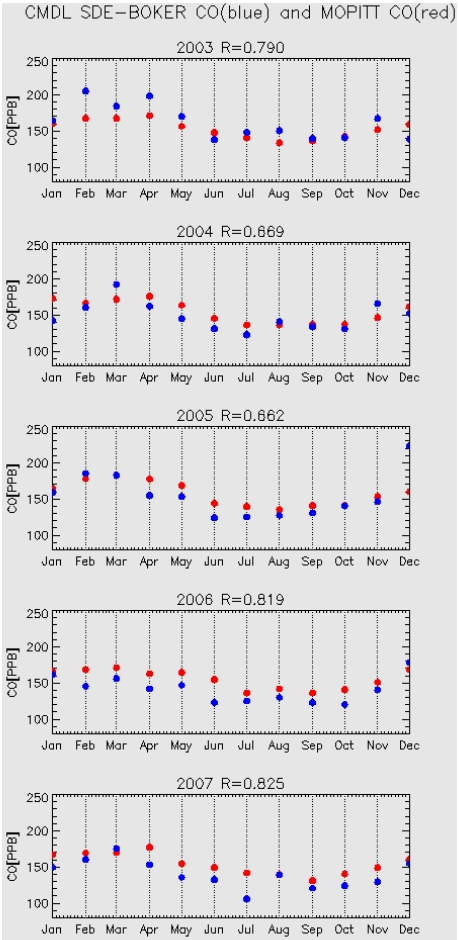

Fig. 6. Comparison of monthly MOPITT CO mixing ratios at 900 hPa retrieval level with GMD flask measurements at Sde-Boker (31.13° N, 34.88° E, 400 m a.s.l.).

ACPD
10, 30893–30925, 2010

European carbon monoxide sources affecting the Eastern Mediterranean

R. Drori et al.

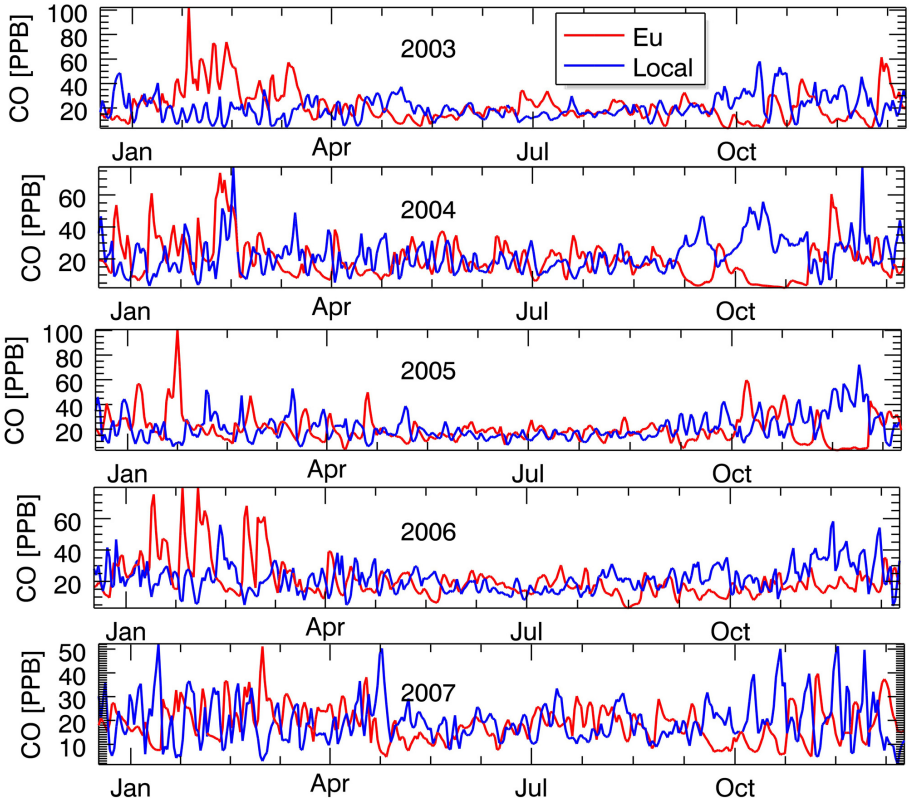

Fig. 7. A comparison between the contribution of European emissions to local CO concentrations (blue) and the contribution of local emissions to local CO concentrations (black). The European contribution is comparable to the local contribution, and they are negatively correlated.

ACPD
10, 30893–30925, 2010

European carbon monoxide sources affecting the Eastern Mediterranean

R. Drori et al.

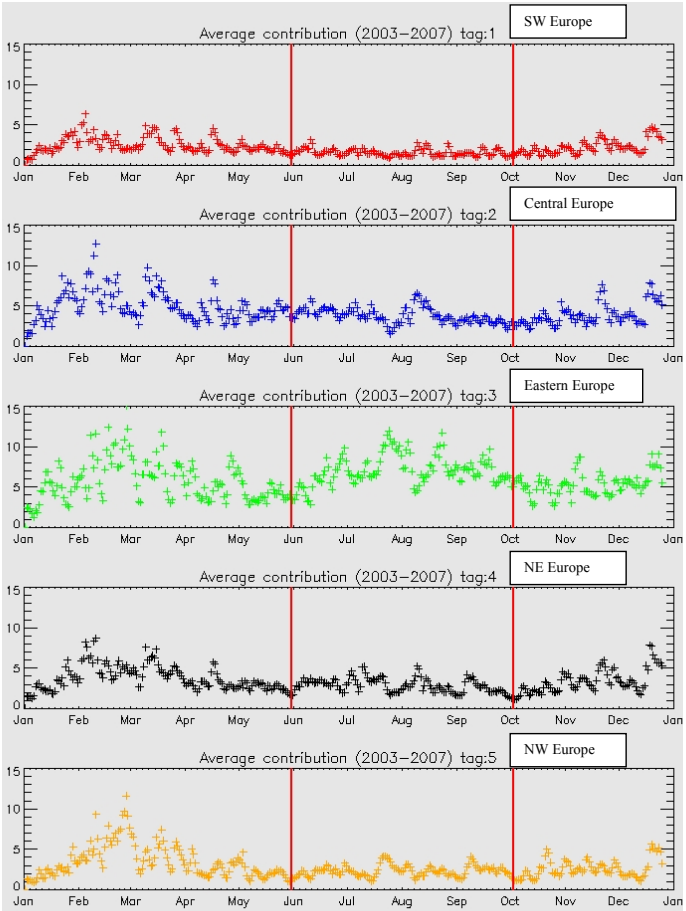

Fig. 8. Average tag contribution (ppb) for the study period (2003–2007). Major episodes can be seen during winter months for all tags.

ACPD
10, 30893–30925, 2010

European carbon monoxide sources affecting the Eastern Mediterranean

R. Drori et al.

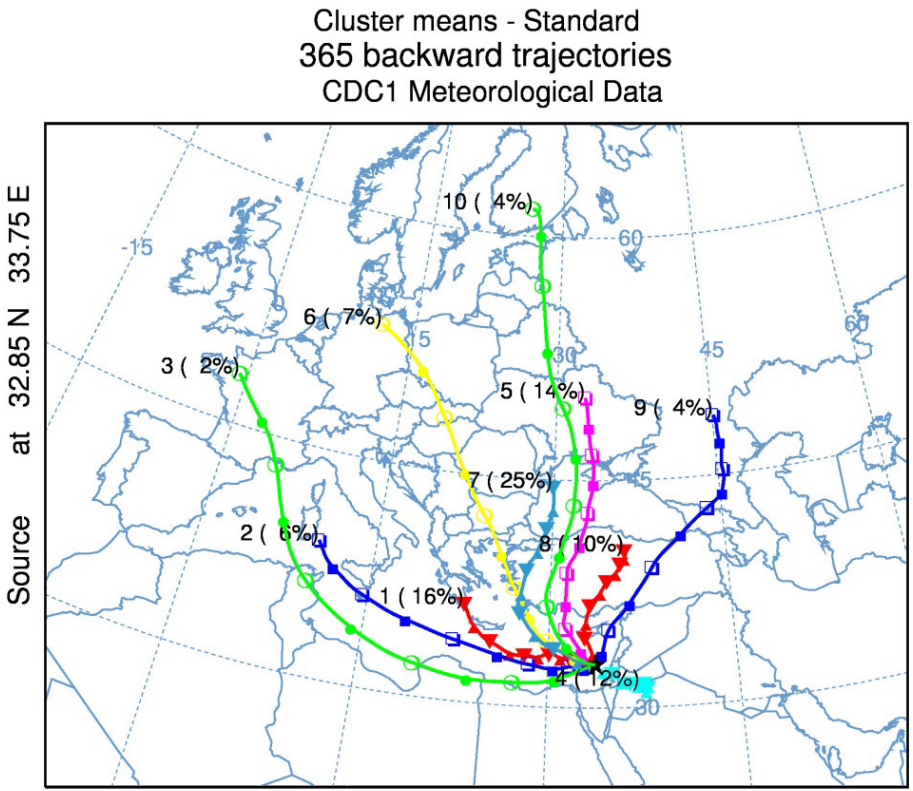

Fig. 9. Five day back-trajectories clusters for 2003. The trajectories were calculated using the HYSPLIT model and were clustered with the HYSPLIT clustering utility.

ACPD
10, 30893–30925, 2010

European carbon monoxide sources affecting the Eastern Mediterranean

R. Drori et al.

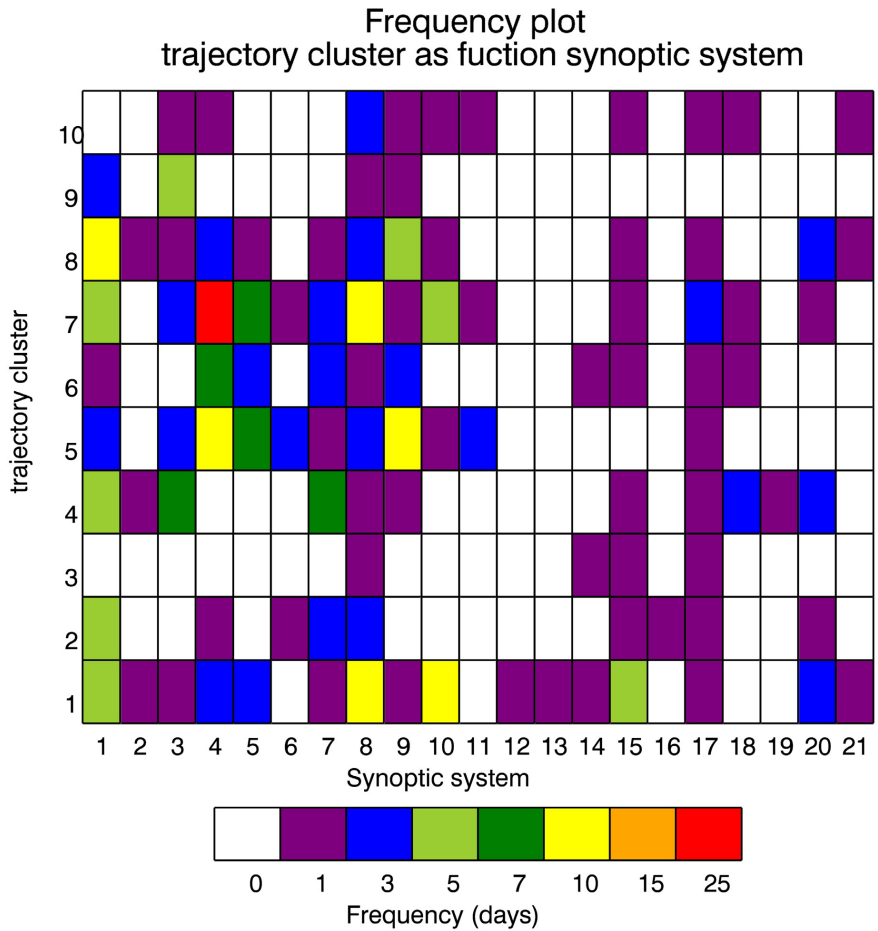

Fig. 10. The frequency (in days) of the combination between synoptic system and back-trajectory cluster for 2003. Synoptic class 0 (undefined) is omitted.

ACPD
10, 30893–30925, 2010

European carbon monoxide sources affecting the Eastern Mediterranean

R. Drori et al.

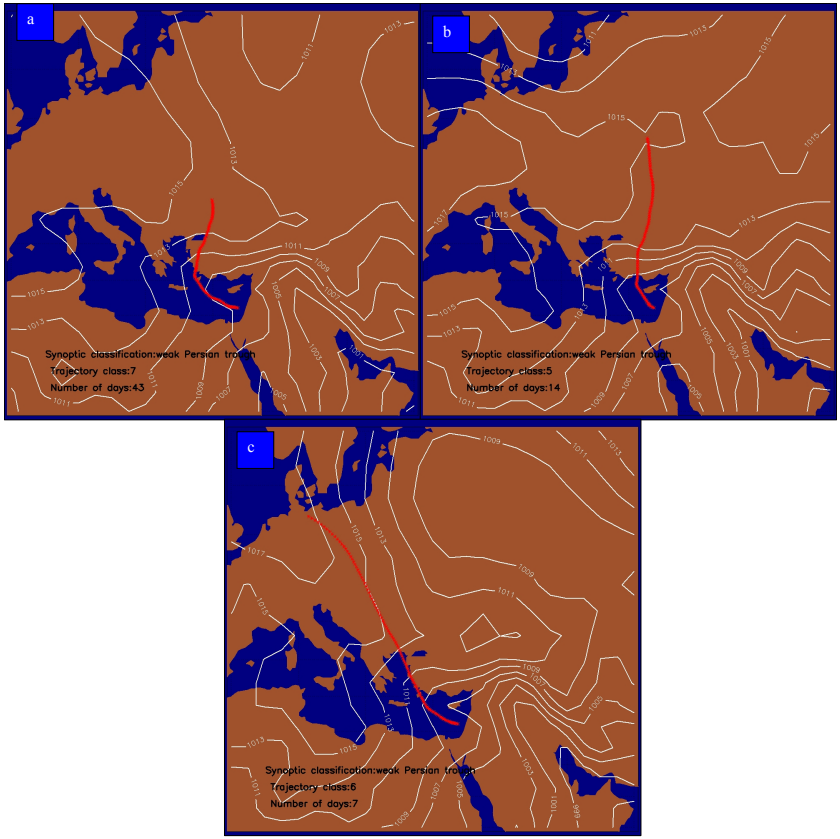

Fig. 11. Three types of weak Persian trough (WPT). Each type is associated with different trajectories (red dots). Sea level pressure (white contours) is averaged for each trajectory cluster. Type **(a)** is associated with 5 day back trajectory cluster 7 from the Balkans (tag 3). Type **(b)** is associated with back trajectory cluster 5 from Eastern Europe (tag 3). Type **(c)** is associated with back trajectory cluster 6 from Western Europe (tag 4).

ACPD
10, 30893–30925, 2010

European carbon monoxide sources affecting the Eastern Mediterranean

R. Drori et al.

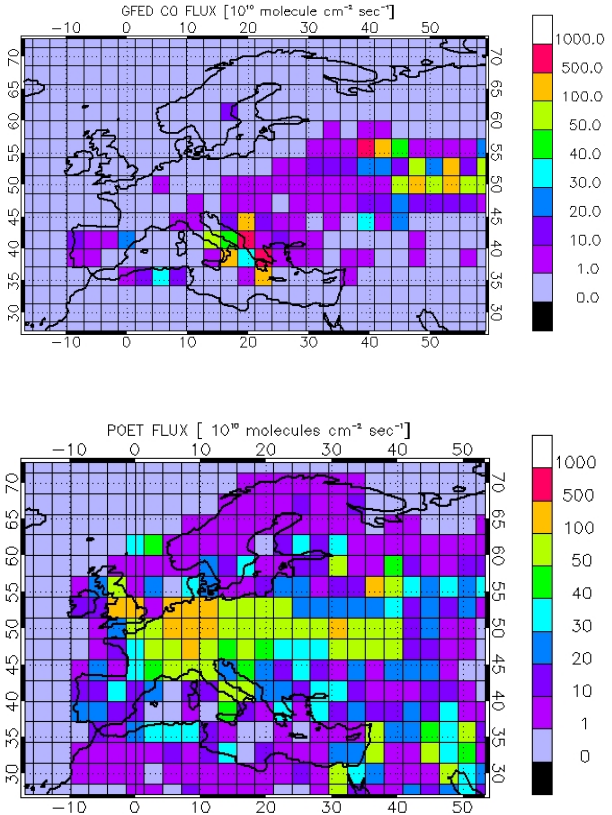

Fig. 12. Biomass burning CO emission fluxes [10^{10} molecules cm^{-2} s^{-1}] from GFED2 for 22 August 2007 (upper panel) and fixed anthropogenic CO emissions from POET [10^{10} molecules cm^{-2} s^{-1}] (lower panel).

ACPD
10, 30893–30925, 2010

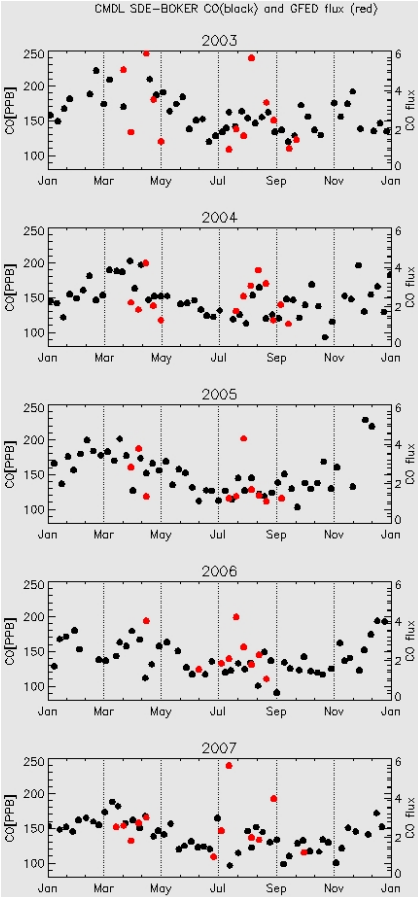

Fig. 13. Local CO surface concentration obtained from NOAA/GMD at Sde-Boker (black circles) and European BB emission fluxes [10^{13} molecules cm^{-2} s^{-1}] calculated from GFED v2 (red circles). Local CO enhancement is synchronized with BB fluxes.

ACPD
10, 30893–30925, 2010

European carbon monoxide sources affecting the Eastern Mediterranean

R. Drori et al.

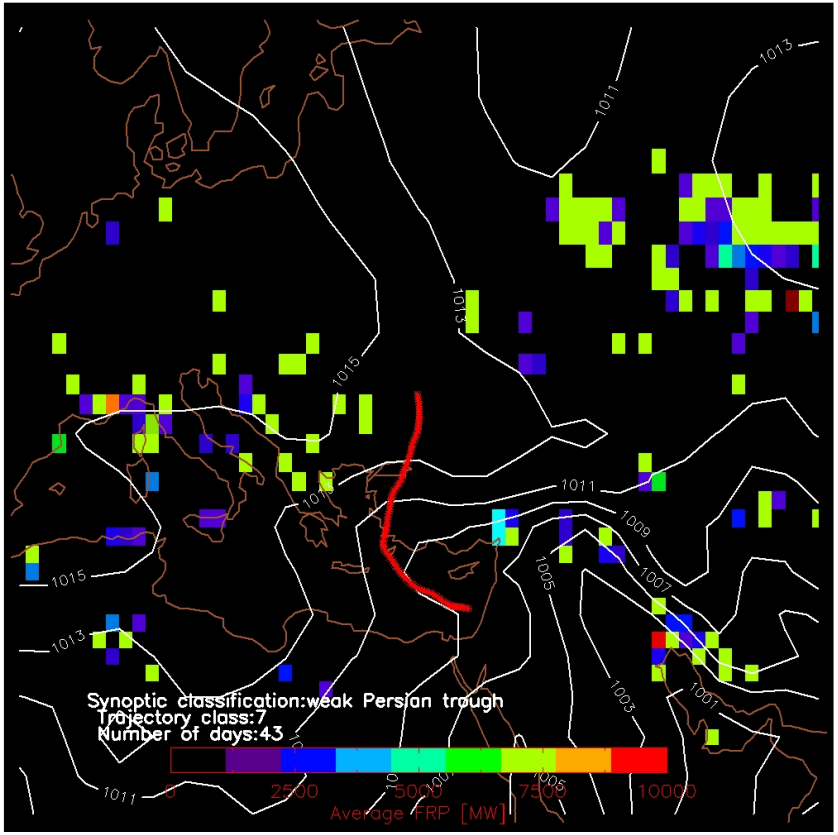

Fig. 14. NCEP/NCAR SLP composite for all days with a weak Persian trough (WPT) and back-trajectory cluster 7 (total of 43 days) along with average FRP [MW] obtained from MODIS active fire. High pressure over Western and Eastern Europe leads to favorable conditions for forest fires there, while Central Europe has less forest fire activity. This synoptic configuration leads to a short back-trajectory from Turkey towards the EM advecting anthropogenic pollution (tag 3) but blocking BB emissions.

ACPD
10, 30893–30925, 2010